A novel target recognition revealed by calmodulin in complex with the basic helix–loop–helix transcription factor SEF2-1/E2-2

GÖRAN LARSSON,[1] JÜRGEN SCHLEUCHER,[1] JACQUELINE ONIONS,[2,3] STEFAN HERMANN,[2,4] THOMAN GRUNDSTRÖM,[2] AND SYBREN S. WIJMENGA[1]

[1]Department of Medical Biosciences, Biophysics, University of Umeå, S-901 87 Umeå, Sweden
[2]Department of Cell and Molecular Biology, University of Umeå, S-901 87 Umeå, Sweden

(RECEIVED July 10, 2000; FINAL REVISION October 31, 2000; ACCEPTED October 31, 2000)

Abstract

Calmodulin is the predominant intracellular receptor for Ca^{2+} signals, mediating the regulation of numerous cellular processes. It can inhibit the DNA binding of basic helix–loop–helix transcription factors by a direct interaction of a novel type. To structurally characterize this novel calmodulin-target interaction, we decided to study the complex of calmodulin with a dimeric peptide corresponding to the DNA-binding domains of the dimeric basic helix–loop–helix transcription factor SEF2-1 (SEF2-1mp) using NMR. Here, we report that the stoichiometry of the calmodulin:SEF2-1mp complex is one dimeric peptide binding two calmodulin molecules. We also report the 1H, 13C, and 15N resonance assignments and the secondary structure of calmodulin in this for NMR large (~38 kD) complex, as well as the 1H assignments and secondary structure of SEF2-1mp. In addition, we determined the amide proton exchange rates of calmodulin and measured intermolecular calmodulin:SEF2-1mp and calmodulin:calmodulin NOE contacts. The isotope-filtered experiments show a large number of SEF2-1mp to calmodulin NOE contacts indicating that a tight complex is formed, which is confirmed by an intermolecular calmodulin:calmodulin NOE contact. The secondary structure and amide proton exchange data show that the binding does not occur via the classical wraparound binding mode. Instead, the data indicate that calmodulin interacts with SEF2-1mp in a more open conformation, although the hydrophobic surfaces of the N- and C-terminal domains still form the main interaction sites. Interactions involving charged residues are also identified in agreement with the known relatively high sensitivity of the binding to ionic strength. Finally, the peptide does not form an α-helix as in the classical wraparound binding mode.

Keywords: Dimer; calmodulin; SEF2-1; NMR; NMR assignment; protein complex

Calmodulin (CaM) is a small (16.7 kD) ubiquitous and multifunctional Ca^{2+} binding protein that plays a central role in the regulation of numerous cellular processes (see Van Eldik and Watterson 1998 and references therein). In accordance with the essential function of calmodulin, the amino acid sequence, and thus the structure, displays an exceptional degree of conservation across species and throughout evolution. The structure of CaM reminds of a dumbbell-shaped molecule with two globular domains connected with a 28–amino acid–long α-helix, called the central helix (Babu et al. 1988; Chattopadhyaya et al. 1992). NMR stud-

Reprint requests to: Sybren Wijmenga, Department of Medical Biosciences, Biophysics, University of Umeå, S-901 87 Umeå, Sweden; e-mail: sybren.wijmenga@chem.umu.se; fax: 46-90-136310.

[3] Present address: ICRF Skin Tumour Labs, Centre for Cutaneous Research, 2 Newark street, London E1 2AT, England.

[4]Present address: Department of Biosciences, Karolinska institutet, Novum, S-141 57 Huddinge, Sweden.

Abbreviations: Baa, basic amphipilic α-helix; bHLH, basic-helix–loop–helix; CaM, Calmodulin; Diamide, Azodicarboxylic acid bis(dimethylamide); NMR, nuclear magnetic resonance spectroscopy; SEF2-1, SL3 enhancer factor 2-1; SEF2-1mp, SL3 enhancer factor -1 mimicking peptide.

Article and publication are at www.proteinscience.org/cgi/doi/10.1110/ps.28401

ies have shown that the central helix is highly flexible with a hinge region from Asp 78 to Ser 81. In fact, NMR relaxation studies suggest that the N- and C-terminal domains almost tumble independently of each other (Barbato et al. 1992). The N- and C-terminal have each two calcium-binding helix–loop–helix motifs, called EF-hands. On calcium binding, the secondary structure of each domain remains essentially the same, but the α-helices undergo a large-scale reorientation. In the apo-state, the two α-helices in the EF-hands are roughly in an antiparallel orientation and form a four-helix bundle-like interior with the other EF-hand in the same domain. On calcium binding, the helices within the EF-hands are more perpendicular, yielding a more open conformation. These calcium-induced rearrangements cause each domain to expose hydrophobic patches suitable for interaction with target proteins (Finn et al. 1995; Kuboniwa et al. 1995; Zhang et al. 1995; Ikura 1996). The calcium affinity of calmodulin is in the range of physiological intracellular calcium levels ($0.1–1 \times 10^{-6}$ M). As a result, most of the calmodulin will be in its apo state in resting cells. When a calcium signal increases the intracellular calcium concentration, calmodulin will bind four calcium ions in a cooperative manner (Waltersson et al. 1993; Van Eldik and Watterson 1998). Thus, the protein acts as a Ca^{2+}-induced molecular switch that allows calmodulin to bind and, thereby, regulate target proteins involved in many important signalling pathways (Houdusse et al. 1996; Van Eldik and Watterson 1998). Several CaM-target interactions that are not Ca^{2+} induced have also been described (Jurado et al. 1999).

In contrast to CaM, whose sequence shows exceptional conservation, the CaM-binding domains of target proteins show extreme sequence variability (Van Eldik and Watterson 1998). Despite the low sequence homology, most calmodulin-binding domains share the property to form basic amphipilic α-helices (so-called Baa helices; O'Neil and Degrado 1990; Ikura et al. 1992; Meador et al. 1992; James et al. 1995). The calmodulin-binding domains are usually stretches of 16–35 amino acids. NMR and crystal structures of calmodulin in complex with synthetic peptides corresponding to the binding domain of skeletal muscle myosin light-chain kinase (M13; Ikura et al. 1992) and chicken smooth-muscle myosin light-chain kinase (Meador et al. 1992) both show the same structural feature. The extended structure of calmodulin collapses into a more compact globule with the two lobes facing each other in a *cis* orientation, creating a hydrophobic tunnel where the peptide binds.

It has been known for a long time that calmodulin can regulate transcriptional activators, but indirectly through CaM-dependent protein kinases and the phosphatase calcineurin (Klee and Krinks 1978; Stewart et al. 1982; Kapiloff et al. 1991; Sheng et al. 1991; Wegner et al. 1992; Dash et al. 1991). However, Corneliussen and coworkers (Corneliussen et al. 1994) have shown that calmodulin can also directly bind to transcription factors belonging to the basic helix–loop–helix (bHLH) family and, thereby, regulate their DNA binding. They also demonstrated that the DNA binding for some bHLH transcription factors were affected by calmodulin, while others where not. They also showed that the bHLH interaction was calcium dependent.

Helix–loop–helix (HLH) proteins are a large family of transcription factors that are important regulators in a multitude of systems. Over 240 HLH proteins have been identified to date in various organisms. HLH factors are intimately involved in control of cell growth and developmental events such as cellular differentiation, lineage commitment, and sex determination. HLH proteins regulate numerous developmental systems including neurogenesis, myogenesis, hematopoiesis, and pancreatic development (Littlewood and Evan 1998; Massari and Murre 2000). Most of the HLH proteins belong to the bHLH group. These transcription factors bind DNA either as homodimers or heterodimers, which increases the range of DNA specificity and transcriptional control from a finite number of transcription factors. The bHLH domain consists of an N-terminal basic region (b) that is immediately N terminal to the helix–loop–helix motif (Ellenberger et al. 1994; Ma et al. 1994). Dimerization occurs in the highly conserved HLH motif where the two HLH domains of the transcription factor together form a left-handed-four-helix bundle. The basic region is by itself responsible for the DNA binding where it binds symmetrically on opposite sides in the major groove of the DNA. The secondary structure of the basic region is α-helical when it is bound to DNA. However, in absence of DNA, the basic region looses its helicity and becomes a very mobile region lacking any well-defined secondary structure (Saudek et al. 1991; Phillips 1994; Fairman et al. 1997). It is also the basic region that makes the calmodulin interaction (Onions et al. 1997).

This was demonstrated by using truncated and chimeric versions of different bHLH proteins (E12, MyoD, and SEF2-1) as well as synthetic peptides spanning different regions of SEF2-1 (also denoted E2-2). To mimic the dimeric features of the bHLH domain, Onions et al. (2000) constructed a peptide spanning the basic region of SEF2-1 that was connected as a dimer through a cysteine linker. This dimeric peptide showed approximately the same calmodulin affinity as the whole bHLH domain of SEF2-1, and a ~80-fold higher affinity than the corresponding monomeric peptide. They showed that the molar ratio between bHLH molecules and calmodulin in the calmodulin:bHLH complex is one calmodulin per bHLH monomer. However, they could not determine whether the stoichiometry was 2 : 2 or if higher multimeric complexes, such as 3 : 3 or 4 : 4, are present. These data showed that the calmodulin: SEF2-1 binding is of a novel type displaying characteristics very different from those of previously characterized calmodulin interactions with monomeric targets.

To structurally characterize this novel calmodulin-target interaction, we decided to study the SEF2-1-mimicking dimeric peptide (SEF2-1mp) interaction with calmodulin by means of NMR. Here we report the stoichiometry of the calmodulin:SEF2-1mp complex. We also report the ^{1}H, ^{13}C, and ^{15}N resonance assignments and the secondary structure of calmodulin in the complex, as well as the ^{1}H assignments and secondary structure of SEF2-1mp. To further characterize the complex, we determined the amide proton exchange rates of calmodulin and measured intermolecular SEF2-1mp-calmodulin NOE contacts as well as intermolecular calmodulin:calmodulin contacts in the dimeric complex. We discuss structural features of the complex based on these data.

Results

Favorable sample conditions were chosen on the basis of the analysis of a series of 2D ^{1}H-^{15}N HSQC spectra recorded on the ^{15}N-labeled calmodulin at different pH, salt conditions, and temperatures. A ^{1}H-^{15}N HSQC spectrum of the complex recorded under the final conditions is shown in Figure 1. The temperature was chosen to be 35°C for two reasons. First, most of the calmodulin:peptide complexes have been assigned at that temperature, which is helpful when CaM:SEF2-1mp has chemical shifts homologous with those of other complexes. Second, severe line broadening caused by conformational exchange was observed at temperatures <25°C, indicating that intermediate-time-scale chemical exchange starts to occur at that temperature.

Stoichiometry

In a titration experiment, increasing amounts of the dimeric SEF2-1mp were titrated into a fixed amount of calmodulin, and a ^{1}H-^{15}N HSQC experiment was recorded for each concentration ratio. From this experiment, the stoichiometry

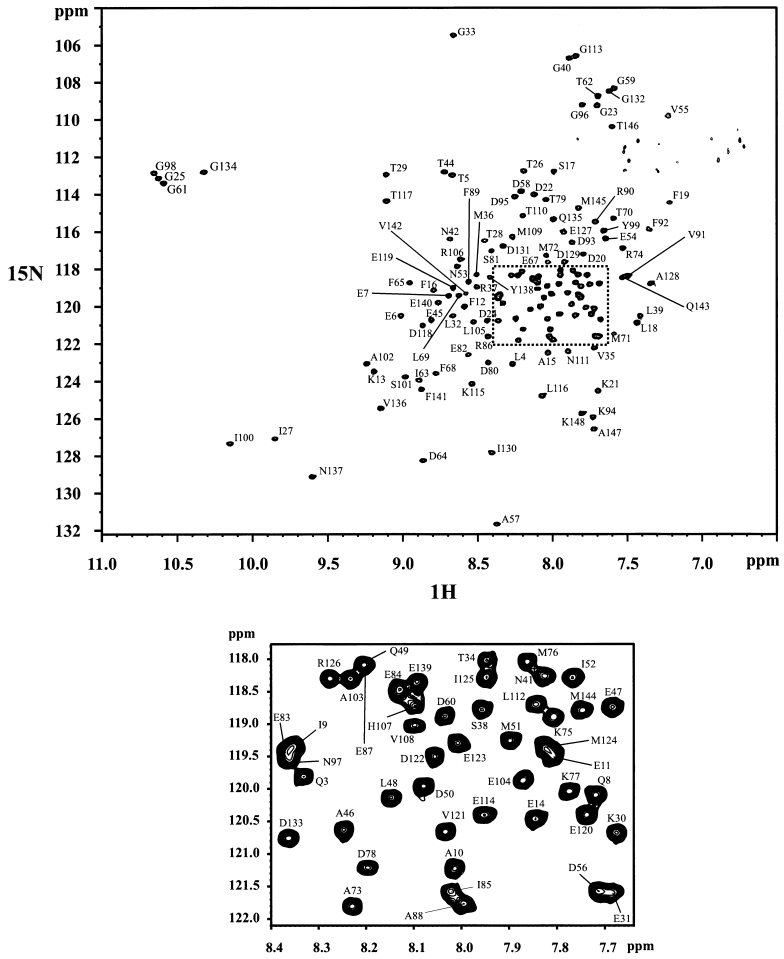

Fig. 1. ^{15}N-HSQC spectrum of the calmodulin:SEF2-1mp complex. The assignment is outlined in the figure. The right panel is an expansion of the most crowded region. The spectrum was recorded on a Bruker DRX 600 spectrometer at 35°C.

of the calmodulin:SEF2-1mp complex was determined to be 1 : 1 (see Fig. 2). In other words, one dimeric peptide binds two calmodulin molecules. During the titration, only one set of calmodulin peaks was observed. This means that the binding is fast on the NMR time scale at the chosen temperature of 35°C.

Assignment of calmodulin and SEF2-1mp

Backbone and sequential assignment of CaM was obtained from the combination of the following triple resonance experiments (Table 2); CBCANH, HNCO, CBCACO(N)H (for a recent review, see Sattler et al. 1999), and CTSL-HCANH (Larsson et al. 1999). The CBCACO(N)H experiment is a slightly modified version of the CBCA(CO)NH experiment (Grzesiek and Bax 1992) that has chemical shift evolution of the carbonyl carbon rather than of the amide nitrogen. This version was selected because the chemical shift dispersion of the CaM:SEF2-1mp complex is better in the carbonyl region than in the amide nitrogen region. Another advantage with carbonyl chemical shift evolution in the CBCACO(N)H is that overlapping resonances in the N, H^N plane of CBCANH can be resolved in the C′, H^N plane of the CBCACO(N)H experiment. The N, H^N plane in the CTSL-HCANH gave both intra- and interresidual C^α resonances, while the CBCANH experiment, with its lower signal to noise ratio, mostly gave the chemical shifts of the intraresidual C^α and C^β carbons. From the same combination of N and H^N shifts, the C′ of the previous residue could be found in the HNCO spectrum. Subsequently, the CBCACO(N)H spectrum was used to find the chemical shifts of the C^α and C^β carbons of the residue N-terminal to the assigned residue. Resonance overlap in the congested C^α region was in most cases resolved with the CTSL-HCANH experiment, which provides much higher C^α resolution than do CBCANH and CBCACONH experiments. The H^α and H^β protons were assigned mainly from the HBHACO(N)H. The residues N-terminal to prolins and residues that for other reasons could not be assigned from the HBHACO(N)H were assigned from the ^{13}C-edited 3D NOESY and/or the ^{15}N-edited 3D NOESY. Assignment of atoms further out n the sidechain was obtained from

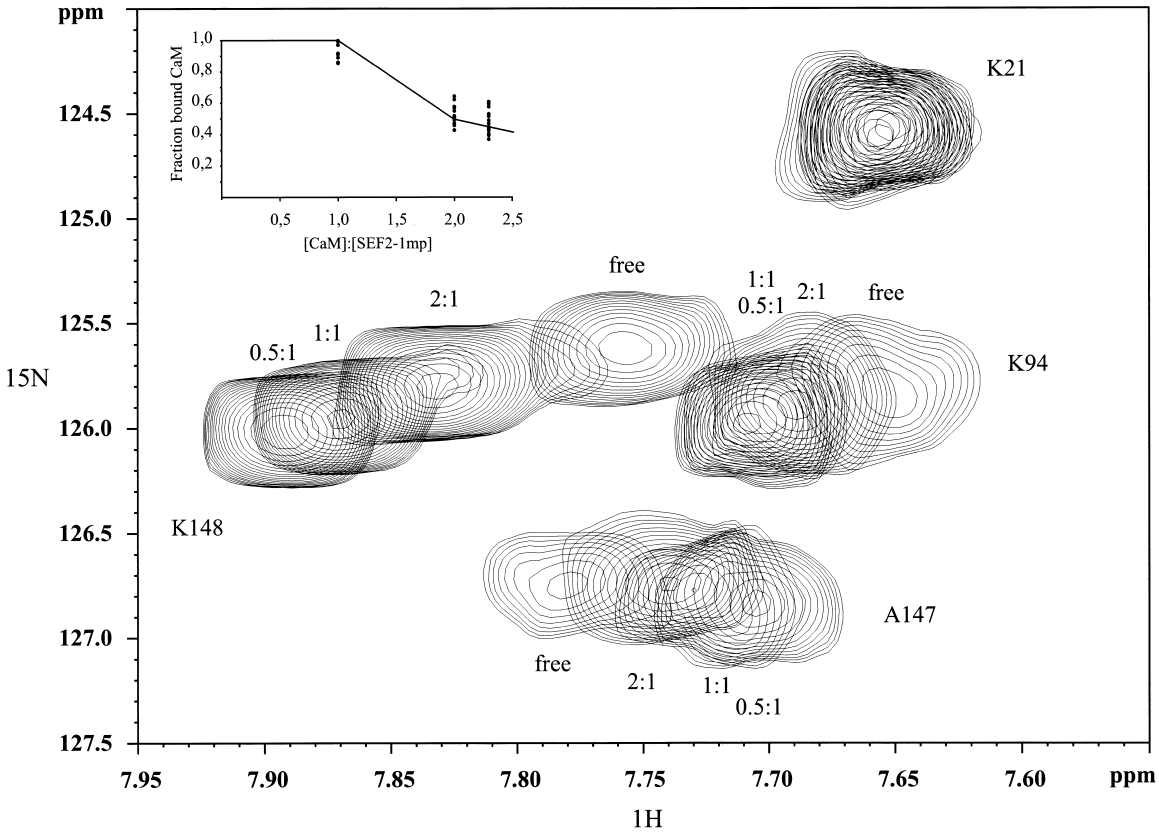

Fig. 2. Expanded regions of four overlaid ^{15}N-HSQC spectra at different calmodulin:SEF2-1mp ratios. The concentration ratios are noted close to the cross peaks. Inserted is a diagram with the fraction bound calmodulin as a function of the calmodulin:SEF2-1 concentration for residues that shifted significantly. The fraction bound calmodulin was determined from the relative change in chemical shifts during the titration. The line in the inserted diagram corresponds to a theoretic titration for a 1 : 1 complex that is in fast exchange.

HC(C)(CO)NH-TOCSY (Montelione et al. 1992) with either 1H or 13C shared-time evolution (Grzesiek and Bax 1993). Because of differences in TOCSY transfer, two different TOCSY mixing times had to be used to assign the main part of the side chains of calmodulin. Sidechain resonances that could not be assigned by the HC(C)(CO)NH-TOCSY, such as the methionine ϵ-CH_3 protons, were assigned by the combination of ^{13}C-edited and ^{15}N-edited 3D NOESY experiments. The aromatic protons in calmodulin were assigned from the (HB)CB(CGCD)HD experiment (Yamazaki et al. 1993) with varying numbers of carbon COSY transfer steps to correlate C^β with either H^δ or H^ϵ. However, the H^ζ protons for the phenylalanines in calmodulin are unassigned because of poor $C^\beta \rightarrow C^\gamma \rightarrow C^\delta \rightarrow C^\zeta$ COSY transfer and their poor shift dispersion in the ^{15}N-edited NOESY. The H^ϵ of His 107 was assigned from the ^{13}C-edited 3D NOESY.

For the ^{1}H assignment of SEF-1mp bound to calmodulin, two-dimensional ^{13}C- and ^{15}N-filtered TOCSY and NOESY experiments were used. Sequence-specific assignment was derived from the ^{13}C- and ^{15}N-filtered 2D NOESY, using interresidue H^N_n-H^N_{n-1} and H^N_n-H^α_{n-1} NOE contacts. The main assignment was achieved at 35°C. However, because of severe overlap and rapid exchange with water, the amide protons of Lys 1 and Glu 2 had to be assigned at 15°C. Sidechain protons of Cys 19 were assigned at 25°C. Because there was no major chemical shift change of SEF2-1mp on calmodulin binding, the sequential assignment of free SEF2-1mp was used as a starting point. For free SEF2-1mp, the crowded proton dimension could be resolved in a natural abundance ^{13}C HSQC (data not shown).

The assignment of ^{1}H, ^{13}C, and ^{15}N of calmodulin and the ^{1}H assignment of the SEF2-1mp have been deposited in BioMagResBank (http://www.bmrb.wisc.edu/) under BMRB accession number BMRB-4310.

$^3JH^NH^\alpha$ coupling constants

From a three-dimensional HNHA spectrum (Vuister and Bax 1993), 128 $^3JH^NH^\alpha$ coupling constants could be determined. The 11 glycines in calmodulin were not taken into account, as the strong dipolar interaction between the two geminal H^α protons gives rise to faster cross-relaxation rates, resulting in underestimated coupling constants. The calmodulin sequence also contains two prolines that lack the HN proton. For the two first residues, no coupling constant could be measured because of incomplete assignment for these residues. Coupling constants for Phe 16, Thr 29, Phe 65, and Thr*138* could not be determined because of the absence of observable H^α cross peaks. This means that their $^3JH^NH^\alpha$ coupling constants are small (<3 Hz), as expected for residues in beginnings of α-helices. The derived $^3JH^NH^\alpha$ coupling constants are displayed in Figure 3B.

ϕ and ψ backbone angles

The chemical shifts of H^α and C^α and, to a lesser degree C^β, C', and N, are good probes for the secondary structure in proteins. It is also well known that the chemical shifts of the protein backbone of homologous proteins show similar patterns. These facts are used in the TALOS software (Cornilescu et al. 1999). TALOS was able to predict 129 out of 148 pairs of ϕ and ψ angles on the basis of the calmodulin assignment. The backbone assignment of Ala 1, Asp 2, and Lys 148 in calmodulin is not complete. Hence, the derivation did not work for these residues. The derivation of ϕ and ψ pairs also failed for residue Asp 20, Gly 23, Gly 40, Pro 43, Gly 59, Met 76, Lys 77, Asp 78, Ser 81, Asp 93, Gly 96, Asn 97, Gly 113, Gly 132, Asp 133, and Thr 146. However, with the exception of Met 76 and Ser 81, these residues are not involved in any regular secondary structure as based on the NOE pattern (Fig. 3A), and the $^3JH^NH^\alpha$ coupling constants (Fig. 3B). In summary, TALOS predicted the ϕ and ψ angles for all eight α-helices and the four short β-strands in calmodulin. The deduced calmodulin backbone angles are shown in Figure 3C.

Secondary structure of calmodulin

Short- and medium-range intramolecular calmodulin NOEs were obtained from the ^{15}N-edited 3D NOESY experiment. Strong or intermediate NOE cross peaks from $H^N_{(i)}$-$H^N_{(i+1)}$), $H^\alpha_{(i)}$-$H^N_{(i+1)}$, and $H^\alpha_{(i)}$-$H^N_{(i+3)}$ characteristic for α-helices helped in the identification of all eight α-helices in calmodulin. The NOE pattern is given in Figure 3A. The small $^3JH^NH^\alpha$-coupling constants for the same residues in combination with the predicted ϕ and ψ backbone angles further confirmed the residues involved in α-helices (Fig. 3B,C). The four β-sheets were mainly identified from the $^3JH^NH^\alpha$ coupling constants, which were ~9 Hz, and the combination of high ψ- and low ϕ-angle. Table 2 contains the identified secondary structure of calmodulin in complex with SEF2-1mp (see the Table 2 legend for the exact criteria used to define a residue as being part of an α-helix or a β-sheet). A comparison with the secondary structure of free calmodulin (Ikura et al. 1991a) as well as the well-characterized calmodulin in complex with a peptide corresponding to skeletal muscle light-chain kinase (M13; Ikura et al. 1992) is also compiled in the same table. Differences in secondary structure with both the CaM and the CaM:M13 complex are marked bold in the table.

Secondary structure of SEF2-1mp

The secondary structure of SEF2-1mp was estimated from the differences of the H^α shifts from their random coil shifts (Wishart et al 1995b), that is, the conformational shifts ΔH^α, and are given in Figure 4. An upfield shift of 0.39 ppm

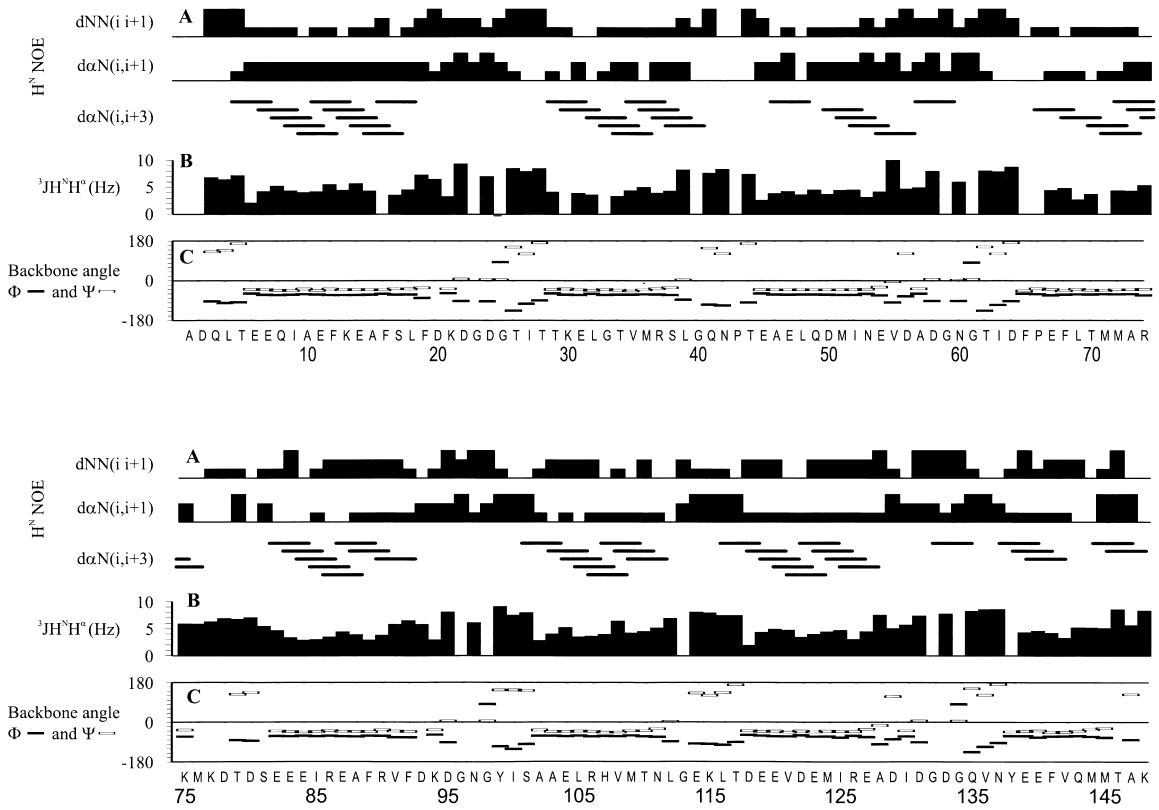

Fig. 3. Summary of the sequential and medium range NOEs involving the H^N and H^α protons (*A*), the $^3JH^NH^\alpha$ coupling constants (Hz; *B*), and from TALOS predicted backbone ϕ and ψ angles (*C*) for calmodulin in complex with SEF2-1mp. For the NOE data, the height of the bar corresponds to the cross-peak intensity (strong, intermediate, or weak). The connectivity between $H^\alpha(i)$ and $H^N_{(i+3)}$ is given by a line between these residues. Missing bars in the $^3JH^NH^\alpha$ coupling constant diagram are either Gly residues, residues with a coupling constant < 2 Hz, or overlapping residues (see Results for exact residues). The filled and open squares in the diagram of predicted backbone angles correspond to the angles ϕ and ψ, respectively. Missing boxes are when the prediction failed (see Results).

or more is found when a residue is involved in an α-helix (Wishart et al. 1991). Remarkably, this was not found for any of the H^α shifts of SEF2-1mp. Furthermore, in the ^{13}C-filtered TOCSY experiment, most of the peptide side-chain resonances could be seen from the amide resonances (data not shown), indicating relatively large $^3JH^NH^\alpha$ coupling constants, which are not found in α-helices. Moreover, the sequential H^N-H^N NOE contacts were relatively strong compared with the intraresidue H^N-H^α NOEs, which again, is in accordance with the fact that the peptide is not purely α-helix. The complete NOE analysis is still in progress. In conclusion, SEF2-1mp does not form a pure α-helix, although some helical tendency can be inferred for residues Asn 7 to Arg 14.

Intermolecular calmodulin:SEF2-1mp contacts

More than 100 intermolecular NOE cross peaks between the calmodulin and the SEF2-1mp have been found in the three-dimensional F1 ^{13}C and ^{15}N-filtered, F2 ^{13}C and ^{15}N-edited NOESY experiment (Zwahlen et al. 1997). A projection along the ^{13}C-dimension in the three-dimensional NOESY is given in Figure 5A, with the possible SEF2-1mp assignment outlined. Strong intermolecular NOEs are found mainly from the methyl groups of L^{13} and V^{15} in SEF2-1mp to hydrophobic residues in calmodulin (Fig. 5B,C), which also include the methyl groups of calmodulin methionines (data not shown). In addition, cross peaks from other SEF2-1mp residues, both hydrophobic and hydrophilic, have been found. Interestingly, relatively strong NOEs are found from the H^δ protons of arginines in SEF2-1mp to calmodulin (Fig. 5D). This means that it is highly likely that electrostatic interactions are present between the basic arginine side chain of SEF2-1mp and the negatively charged calmodulin surface. A complete assignment of the NOESY spectrum is presently ongoing. Because of the high symmetry of the two globular domains in calmodulin and the relatively poor resolution in the three-dimensional isotope-filtered NOESY, only a small number of NOEs have been unambiguously assigned so far based on chemical shift positions alone. The remaining NOEs have to be assigned in an iterative way during the structure calculation.

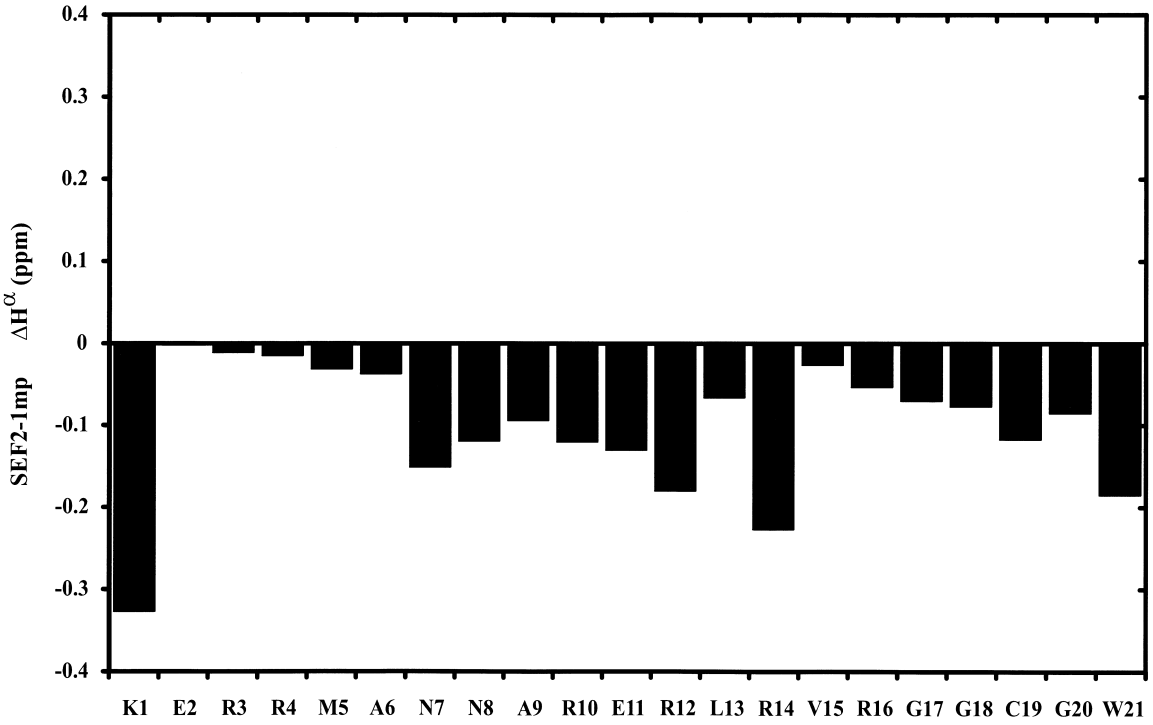

Fig. 4. Difference between experimental H^{α} shift and the random coil H^{α} chemical shifts of calmodulin-bound SEF2-1mp. The H^{α} chemical shifts of the calmodulin-bound SEF2-1mp are not shifted up-field sufficiently to be involved in an α-helix. Thus, the SEF2-1mp does not have any regular secondary structure when it is bound to calmodulin.

Intermolecular calmodulin:calmodulin contacts

From a three-dimensional F1 ^{13}C and ^{15}N-filtered, F2 ^{13}C and ^{15}N-edited NOESY experiment, with a mixture of double-labeled and unlabeled calmodulin, one calmodulin: calmodulin contact has so far tentatively been identified. This contact is between Met 36 ϵ-CH_3 in one calmodulin and the δ-CH_3 in Leu 112 in the other calmodulin (see Materials and Methods).

Hydrogen exchange

The apparent exchange rates, R_{ex}*, of H^N protons in calmodulin in complex with SEF2-1mp were determined at pH 6.0 from the ^{15}N-edited NOESY (see Materials and Methods). The R_{ex}* values are given in Table 3, together with the exchange rates, R_{ex}, determined for free calmodulin and the calmodulin:M13 complex (Spera and Ikura 1991). From Table 3 it becomes apparent that several amide protons in the calmodulin:SEF2-1mp complex have exchange rates that differ from both free calmodulin and the calmodulin:M13 complex. For residues with the H^{α} proton close to the water resonance (Leu 4, Asp 58, Asn 60, Asp 78, Asp 80, and Asn 97), the apparent exchange rates calculated from a NOESY spectrum can be misleading because of additional NOE transfer leading to a possible overestimation of R_{ex}*. They are, therefore, excluded except for Asp 78 and Asp 80, which were in the hinge region. For the threonine and serine residues with hydroxyl groups in their side chains, significant NOE transfer from the H^N to the hydroxyl group may occur, also resulting in overestimated apparent exchange rates (Spera and Ikura 1991). This could explain the increased exchange relative to free calmodulin and calmodulin:M13 seen in Table 3 for all the threonine and serine residues as well as their α-helix neighbors Gln 8, Glu 47, and Glu 120. For other residues, the exchange rate can also be overestimated, but only slightly, as described in Materials and Methods. Because the increased apparent exchange rates in the calmodulin:SEF2-1mp, relative to free calmodulin and calmodulin:M13, may be attributed to NOE effects (see Materials and Methods), we will concentrate on residues that show decreased exchange rates. In particular, the residues in the loop/hinge region (Lys 75 to Glu 82) all show decreased exchange rates in comparison with both free calmodulin and calmodulin:M13. This is interesting because for the calmodulin:M13 complex, a drastic increase in exchange rate is observed in this region.

Discussion

We have obtained the resonance assignment and determined the secondary structure together with other structural pa-

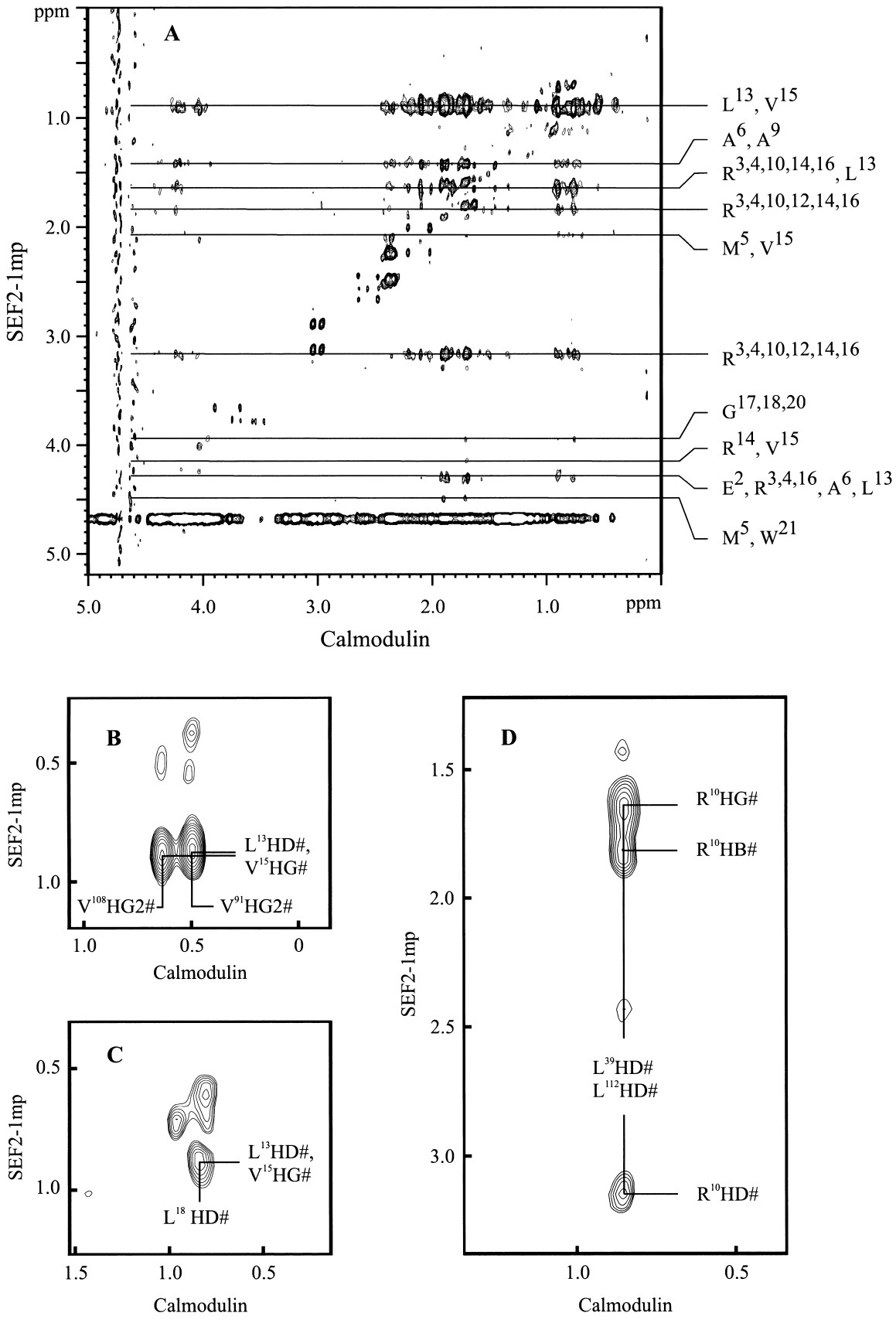
A
ppm
SEF2-1mp
Calmodulin
L13, V15
A6, A9
R3,4,10,14,16, L13
R3,4,10,12,14,16
M5, V15
R3,4,10,12,14,16
G17,18,20
R14, V15
E2, R3,4,16, A6, L13
M5, W21
B
L13HD#,
V15HG#
V108HG2#
V91HG2#
C
L13HD#,
V15HG#
L18 HD#
D
R10HG#
R10HB#
L39HD#
L112HD#
R10HD#

rameters of calmodulin and SEF2-1mp in the calmodulin:SEF2-1mp complex as a model system for the natural calmodulin:SEF2-1 interaction. SEF2-1 is a basic helix–loop–helix transcription factor, which binds as a dimer to DNA via its two basic helices. When interacting with calmodulin, each of the basic DNA-binding domains binds one calmodulin. To mimic the SEF2-1 dimer as closely as possible, the peptide sequence of SEF2-1mp was taken identical to the basic region of SEF2-1. The linker region in SEF2-1mp was designed to closely match the distance between the C termini of the basic regions in the dimeric bHLH transcription factors E47 and MyoD (Ellenberger et al. 1994; Ma et al. 1994). Binding studies by Onions et al. (2000) have shown that dimer formation significantly increases the binding constant of the SEF2-1mp for calmodulin and that the SEF2-1mp dimer and SEF2-1 have approximately the same binding constant for calmodulin. Moreover, the SEF2-1mp binding shows a similar salt dependence as that of SEF2-1 binding. In conclusion, the dimeric SEF2-1mp indeed closely mimics the natural dimeric target SEF2-1.

Most of the calmodulin:peptide complexes studied so far are monomeric. However, Yuan and Vogel (1998) have recently reported on a calmodulin–Petunia Glutamate Decarboxylase (PGD) complex, where, via fluorescence analysis, it is shown that the single Trp residue of the peptide becomes bound to both the N- and C-terminal lobes of calmodulin. These results predict binding of one calmodulin to two PGD molecules, which leads to dimerization of the PGD protein. The unique feature of the calmodulin interaction with SEF2-1mp is that one dimeric SEF2-1mp binds two interacting calmodulins. This is based on the stoichiometrical analysis by Onions et al. (2000) as well as our titration experiments and our finding of intermolecular calmodulin:calmodulin interactions (Met 36 in the N-domain of one calmodulin to Leu 112 in the C-domain of the other calmodulin). In other words, a 38-kD complex is formed that is large for NMR studies. Nevertheless, high-quality NMR spectra were obtained that allowed for complete resonance assignment and even determination of intermolecular NOE contacts. Relaxation studies, to be reported elsewhere, show that T2 relaxation times are shorter than in the calmodulin:M13 complex in agreement with a nonspherically shaped dimeric complex.

The dimeric nature of the calmodulin:SEF2-1mp complex is expected to affect the structure of calmodulin as compared to that in the monomeric calmodulin:peptide complexes. The monomeric peptide complexes for which the X-ray structure (e.g., Meador et al. 1992; Mirzoeva et al. 1999) or the NMR structure (e.g., Ikura et al. 1992; Osawa et al. 1999) have been determined share the following structural features: First, the tertiary backbone structure of the N- and C-terminal domain of calmodulin is well conserved. In addition, no significant structural changes occur in the tertiary backbone structure of the individual domains on peptide binding, as follows from a comparison with the structure of free calmodulin (Babu et al. 1988). Structural differences are found with regard to the conformation of the side chains on the binding surfaces. Second, on peptide binding, the N- and C-terminal domains of calmodulin reorient and clamp around the α-helical target peptide (Ikura et al. 1992; Meador et al. 1992), which is sometimes partly folded back on itself (Osawa et al. 1999). This is called the wraparound binding mode.

The recently published structure of the 20-residue-long peptide C20W, from the plasma membrane calcium pump, in complex with calmodulin is different. Here, the C20W binds solely to the C-terminal lobe of calmodulin (Elshorst et al. 1999). Most interesting, the tertiary backbone structure of the C-domain of calmodulin is again very similar to that of the C-terminal domain in the wraparound complexes.

The reorientation of the N- and C-terminal calmodulin domains observed in these monomeric complexes on peptide binding is possible because the N- and C-terminal domains in free calmodulin are connected via a flexible linker (ranging from Asp 78 to Ser 81), which extends on binding to the target peptide (from Arg 74 to Ser 81). These structural characteristics are reflected in the secondary structure and amide proton exchanges rates. A comparison of the reported secondary structure data on calmodulin complexes with those presented here can thus give insight into the structural characteristics of the calmodulin:SEF2-1mp complex.

To reliably define the regions of secondary structure of calmodulin in the calmodulin:SEF2-1mp complex, we com-

Fig. 5. An expanded region of the projection along the ^{13}C axis (F2) in the three-dimensional F1 ^{13}C- and ^{15}N-filtered, F2 ^{13}C- and ^{15}N-edited NOESY spectrum (*A*) and some selected carbon planes of the three-dimensional NOESY spectrum (*B*,*C*,*D*). The projection in panel A is expanded to only show the H^{α} and side-chain protons in the calmodulin (F3) and SEF2-1mp proton dimensions (F1). Tentative SEF2-1mp assignments are outlined in the spectrum. Panel B is an expanded region of a carbon plane that corresponds to the CG2 chemical shift of Val108 (20.8 ppm) in calmodulin. The panel shows hydrophobic contacts between the C-terminal of calmodulin and SEF2-1mp, that is, from the HG2 protons of Val 91 and Val 108 in calmodulin to the HD protons of Leu 13 and/or the HG protons of Val 15 in SEF2-1mp. Panel C is an expanded region of a carbon plane that corresponds to the two-CD carbon chemical shift of Leu 18 (24.2 ppm) in calmodulin. The panel shows hydrophobic contacts between the N-terminal of calmodulin and SEF2-1mp, that is, from the HD protons of Leu 18 in calmodulin to the HD protons of Leu 13 and/or the HG protons of Val 15 in SEF2-1mp. Panel D is an expanded carbon plane (25.6 ppm) and displays contacts between the HB, HG, and HD protons of Arg 10 in SEF2-1mp to the Leu 39 and/ Leu 112 in calmodulin.

Table 1. *Parameters for NMR experiments used to assign the $^{1}H/^{13}C/^{15}N$ resonances for calmodulin in the calmodulin:SEF2-1mp complex*

	^{1}H				D2				D3					
Experiment	SW[g]	N*[h]	Carrier[c]	Nucleus	SW[g]	N*[h]	Carrier[c]	Nucleus	SW[g]	N*[h]	Carrier[c]	Matrix dimension[d]	Number of scans[e]	Mixing time[f]
CBCANH[a,j]	3180	800	8.79	^{15}N	1277	56	118.3	^{13}C	9055	110	45.3	1024 × 128 × 256	48	
CBCACO(N)H[a]	3180	800	8.79	^{13}C	1207	54	177.3	^{13}C	9055	110	45.3	1024 × 128 × 256	24	
HNCO[a,j]	3180	800	8.79	^{15}N	1277	62	118.3	^{13}C	1207	116	177.3	1024 × 256 × 256	8	
HBHACO(N)H[a]	4006	1024	8.79	^{1}H	4026	144	2.90	^{13}C	1207	54	177.3	1024 × 256 × 128	16	
CTSL-HCANH[a,j]	5252	1024	8.79	^{15}N	1399	62	118.5	^{13}C	3632	170	54.0	1024 × 128 × 512	16	
^{15}N edited 3D NOESY[a,j]	9470	2048	8.79	^{1}H	7564	128	4.70	^{15}N	1295	80	118.0	2048 × 512 × 256	24	100
^{13}C edited 3D NOESY[a,j]	4006	1024	4.70	^{1}H	7564	128	3.00	^{13}C	8048	100	42.4	1024 × 256 × 256	24	120
^{13}C edited HSQC[a]	4528	1024	7.00	^{13}C	1660	42	126.5							
(HB)CB(CGCD)Hd[a]	4528	1024	7.00	^{13}C	6345	154	136.0							
(H)C(C)(CO)NH TOCSY[b,j]	6335	1024	4.70	^{15}N	1166	50	118.8	^{13}C	8048	100	42.4	1024 × 128 × 128[i]	32	13.8
(H)C(C)(CO)NH TOCSY[b,j]	6335	1024	4.70	^{15}N	1166	50	118.8	^{13}C	8048	100	42.4	1024 × 128 × 128[i]	32	20.7
H(CC)(CO)NH TOCSY[b,j]	6335	1024	4.70	^{15}N	1166	50	118.8	^{1}H	3344	78	2.91	1024 × 128 × 256[i]	32	13.8
H(CC)(CO)NH TOCSY[b,j]	6335	1024	4.70	^{15}N	1166	50	118.8	^{1}H	3344	78	2.91	1024 × 128 × 256[i]	32	20.7

[a] Experiments recorded at ^{1}H frequency of 600 MHz.
[b] Experiments recorded at ^{1}H frequency of 500 MHz.
[c] Carrier position in ppm.
[d] Final processed matrix size in real points.
[e] Number of scans collected per FID.
[f] Mixing time (ms), in case of TOCSY half of the mixing time is taken up by ROE compensation delays.
[g] Sweep width (Hz).
[h] Number of complex points in this dimension.
[i] The spectra were processed with 2048 real points prior to discarding the aliphatic region.
[j] The experiment uses gradient enhancements (Kay et al. 1992; Schleucher et al. 1994). All ^{1}H dimensions were referenced to internal DSS. ^{13}C and ^{15}N dimensions were calibrated using the known magnetogyro ratios (Wishart et al. 1995).

bined all the information from $^3JH^NH^\alpha$ coupling constants and the predicted ϕ and ψ backbone angles and short- and medium-range NOEs, C^α-chemical shifts (Fig. 3). The secondary structure elements derived in this way are given in Table 2. As can be seen, in the calmodulin:SEF2-1mp complex the secondary structures of the N- and C-terminal domains are basically the same as for free calmodulin and the calmodulin:M13 complex. This strongly suggests that, as for the other peptide complexes, the domains do not change their tertiary backbone structure on binding to SEF2-1mp. This does not imply that the conformations of the side chains in the binding surface are similar to that in the calmodulin:M13 complex or the other complexes.

The orientation of the N- and C-terminal domains in calmodulin affect the region in and around the flexible hinge region (Met 72 to Glu 83). Hence, the secondary structure and amide proton exchange rates in this region reflect the domain orientation. Comparison of the secondary structure of this region in free calmodulin (Ikura et al. 1991a), calmodulin:M13 (Ikura et al. 1991b; Ikura et al., 1992), and calmodulin:SEF2-1mp shows interesting differences (Table 2). On formation of the calmodulin:M13 complex, the hinge region in free calmodulin (residues 78–81) is extended into a flexible loop ranging from Arg 74 to Glu 82. This extension of the hinge region is observed for all known calmodulin:peptide complexes. In the calmodulin:SEF2-1mp complex, this extension of the hinge region is not observed. Instead, the hinge region starts at residue 77 and ends at residue 80. In other words, the hinge region is quite similar but slightly shifted compared to that of free calmodulin. These findings are evidenced by the following data. From Met 72 to Glu 83 the ΔC^α shifts of calmodulin:SEF2–1mp closely follow those of free calmodulin, while those of calmodulin:M13 are significantly different (Fig. 6). From Met 72 to Met 76, the ΔC^α shifts of both free calmodulin and calmodulin:SEF2-1mp complex are larger than zero, indicating the presence of helix IV up to residue 76. In contrast, the ΔC^α shifts of calmodulin:M13 are smaller than zero for these residues, indicating that the helix is disrupted because of the wraparound binding mode. Furthermore, the amide protons of Ala 73 to Met 76 in the calmodulin:SEF2-1mp complex are strongly protected against hydrogen exchange (Table 3). The amide protons of Lys 75 and Met 76 are more protected not only compared with the calmodulin:M13 complex but even compared with free calmodulin. This indicates that these amide protons form more stable hydrogen bonds than in free calmodulin and suggests that helix IV in calmodulin:SEF2-1mp is stabilized with respect to helix IV in free calmodulin. This stiffening of helix IV rules out the wraparound binding mode as found in the

Table 2. *Identified secondary structure in calmodulin:SEF2-1mp complex, free calmodulin (Ikura et al. 1991a) and calmodulin:M13 complex (Ikura et al. 1991b; Ikura et al., 1992)*

	Residue range		
Secondary structure	CaM:SEF2-1mp[a]	CaM:M13	CaM
Helix I	6–19	7–19	6–19
Helix II	29–38	29–38	29–38
Helix III	45–54	45–54	45–54
Helix IV	**65–76**[b]	**65–73**[b]	**65–77**
Helix V	**81**[c]**–92**	**83**[c]**–93**[d]	**82**[c]**–93**[d]
Helix VI	102–111	102–111	102–111
Helix VII	118–127	118–127	118–127
Helix VIII	138–144	138–146[e]	138–146[f]
Strand I	26–28	26–28	26–28
Strand II	63–65	63–65	63–65
Strand III	99–101	99–101	99–101
Strand IV	135–137	135–137	135–137

[a] Residues were defined to be in an α-helix when ΔC^α was >0.8 ppm for three residues in a row, the ϕ and ψ angles, predicted from TALOS, were smaller than −10° for these residues, the $^3JH^NH^\alpha$ coupling constants smaller than 6 Hz, and the $\alpha N(i,i+3)$ NOE contacts are present. The β-strand regions were defined based on the ϕ and ψ angles ($\phi < -90$ and $\psi > 20$) and $^3JH^NH^\alpha$ coupling constants larger than 7 Hz.

[b] Although no data for the ϕ and ψ angles are available for Met[76], the ΔC^α chemical shifts, the $\alpha N(i,i+3)$ NOE contacts, and the $^3J(H^NH^\alpha)$ <6Hz indicate that the helix ends at Met[76]. For the calmodulin:M13 the $NN(i,i+1)$ indicates that helix IV continues to Arg74, whereas the ΔC^α, $\Delta C'$, and ΔH^α suggest that the helix already ends at Met[71] (Ikura et al. 1991b).

[c] Although no data for the ϕ and ψ angles are available, the ΔC^α chemical shifts, the $NN(i,i+1)$ NOE contact, the $\alpha N(i,i+3)$ NOE contact, and the $^3J(H^NH^\alpha)$ <5Hz indicate that the helix starts at residue 81 for calmodulin:SEF2-1mp. In the free calmodulin the $NN(i,i+1)$ NOE contact and $\alpha N(i,i+3)$ NOE contact are absent for Ser81 and $\Delta C^\alpha < 0.8$ ppm. Therefore helix V starts at Glu[82]. For the calmodulin:M13 complex helix V is stated to start at Glu[83] based on the still relatively high exchange rate of Glu[82] (Ikura et al. 1991b; Ikura et al. 1992), although the NN(82,83) NOE contact is present and the $\Delta C^\alpha > 0.8$ ppm for Glu[82]. Thus, the helix could also start at Glu[82]. Note that no NN(81,82) NOE contact is present.

[d] Based on the ΔC^α chemical shifts criterion the helix should stop at residue 92.

[e] Based on the ΔC^α chemical shifts the helix ends at residue 144 as ΔC^α for residue 145 is <0.

[f] Based on the ΔC^α chemical shifts criterion the helix ends at residue 144.

Significant differences in secondary structure are indicated in bold.

Table 3. *Apparent exchange rate for the calmodulin:SEF2-1mp complex and a comparison with the calmodulin:M13 complex and free calmodulin (Spera et al. 1991)*

Residue	Cam:SEF2-1mp (s^{-1})	CaM:M13[a] (s^{-1})	Calmodulin[a] (s^{-1})
T5	*3.6*	*<0.1*	*<0.1*
E7	1.0	<0.1	1.0
Q8	1.3	<0.1	<0.1
I9	0.5	0.6	<0.1
S17	*0.3*	*<0.1*	*<0.1*
T26	*0.6*	*<0.1*	*<0.1*
T28	*0.3*	*<0.1*	*<0.1*
T29	*0.7*	*0.6*	*1.2*
K30	1.5	2.5	3.1
E31	0.3	<0.1	<0.1
T34	*0.9*	*<0.1*	*0.2*
S38	*0.4*	*<0.1*	*<0.1*
G40	**0.1**	**2.1**	**2.3**
N42	**5.2**	**15.0**	**12.0**
T44	*2.6*	*<0.1*	*<0.1*
E45	2.7	1.1	2.3
A46	1.2	0.6	1.1
E47	1.2	<0.1	<0.1
T70	*0.6*	*<0.1*	*<0.1*
A73	0.1	<0.1	<0.1
R74	0.1	0.1	0.1
K75	**<0.1**[c]	**2.6**	**0.5**
M76	**0.3**	**1.7**	**1.6**
K77	**0.7**	**7.2**	**2.6**
D78[b]	**2.8**	**13.0**	**6.3**
T79	***3.1***	***13.0***	***7.7***
D80[b]	**2.2**	**4.2**	**6.6**
S81	***4.3***	***13.0***	***13.0***
E82	**2.6**	**4.2**	**4.3**
E83	0.4	0.2	0.4
E84	0.4	0.3	<0.1
A103	0.5	0.8	1.7
E104	1.0	<0.1	<0.1
T110	*1.0*	*<0.1*	*0.3*
N111	0.4	<0.1	<0.1
L112	0.2	<0.1	1.1
G113	0.1	<0.1	1.0
E114	0.1	<0.1	0.9
K115	**0.7**	**1.6**	**1.5**
L116	0.1	0.5	0.1
T117	*0.8*	*<0.1*	*<0.1*
D118	2.5	2.1	3.6
E119	1.1	0.8	0.5
E120	1.1	<0.1	<0.1
T146	*1.2*	*<0.1*	*0.1*
A147	**0.4**	**6.5**	**2.4**
K148	<0.1	0.6	0.1

[a] To be able to compare our data with exchange rates for free calmodulin and calmodulin in complex wth the M13 peptide determined by Spera et al. (1991) at pH 7.0, their exchange rates were scaled down with a factor 10. Threonine and serine residues can have NOE transfer to the H^N protons from the hydroxyl group in their sidechains. These residues are marked with italic test.

[b] Residues with H^α close to the water frequency (see Materials and Methods). Residues that show significant protection from hydrogen exchange in the CaM:SEF2-1mp complex compared with CaM:M13 and free CaM are marked with bold text.

[c] Assuming that the minimum detectable intensity of the cross peak at the H_2O line is 1% of that of the diagonal.

calmodulin:M13 complex. A second interesting feature is that the NOE data indicate that helix V already starts at Ser 81, which is one residue earlier than in free calmodulin and one or two residues earlier than in the calmodulin:M13 complex (Table 2). In free calmodulin as well as in the wraparound model, this residue is part of the flexible hinge/loop region. The amide proton of Ser 81 is one of the most strongly exchanging protons in both the free calmodulin and the calmodulin:M13 complex (Table 3). In the calmodulin:SEF2-1mp complex, the exchange is reduced by a factor of three, consistent with the other NOE data and indicating that Ser 81 is part of the helix. Note that the amide protons of other residues in the hinge region (Lys 77 to Asp 80) are also more protected against exchange than in free calmodulin (Table 3). We therefore conclude that the binding mode of SEF2-1mp differs from that of M13. In particular, the hinge region is not extended as in the wraparound binding mode. Instead, the stabilization of the end of helix IV and the beginning of helix V suggests that the domains may be configured in a more open orientation compared with the wraparound binding mode.

In the wraparound binding mode, the target peptide is α-helical and anchors the N and C termini of calmodulin via hydrophobic residues spaced eight or 12 residues apart (Ikura et al. 1992; Meador et al. 1992; James et al. 1995). A spacing of 14 residues, as has been observed in the CaM:CaMKK complex (Osawa et al. 1999) is also compatible with the wraparound binding. However, in the CaM:CaMKK complex, the peptide binds in the reverse direction, compared to the calmodulin:M13 complex. Figure 4 shows the conformational ΔH^α shifts of SEF2-1mp when bound to calmodulin. None of the conformational ΔH^α shifts are more negative than −0.39 ppm, the criterion defined by Wishart for residues in an α-helix (Wishart et al. 1991). This indicates that most of the peptide is not in an α-helical conformation, although some helical tendency can be observed from Asn 7 to Arg 14. This putative α-helix is too short to anchor both the N- and C-terminal domains of calmodulin as in the binding modes described above. Furthermore, SEF2-1mp does not contain hydrophobic residues spaced 8, 12, or 14 residues apart. We conclude that the calmodulin:SEF2-1mp interaction also differs from other calmodulin:peptide interactions in that SEF2-1mp is not in a pure α-helical conformation.

In the wraparound binding mode, the hydrophobic surfaces of the N- and C-terminal domains face each other and form a hydrophobic tunnel. We investigated whether the calmodulin residues that interact with SEF2-1mp reside on the same hydrophobic surfaces, despite the fact that the binding is not of the wraparound type. In the calmodulin X-ray structure determined by Chattopadhyaya et al. (1992), we located the calmodulin residues with the largest chemical shift differences between free calmodulin and calmodulin:SEF2-1mp (Fig. 7). We defined a residue as being af-

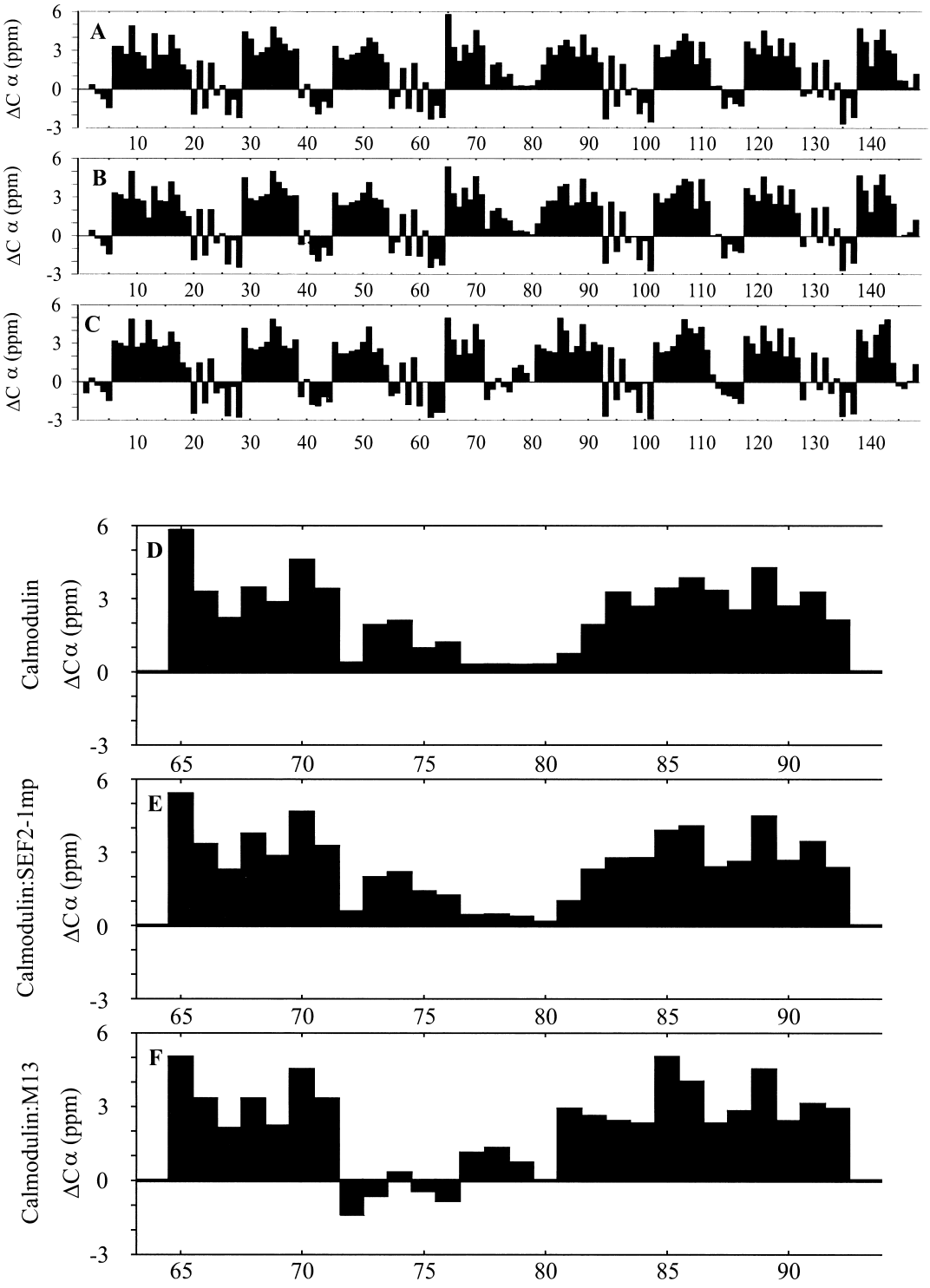

Fig. 6. The differences between the experimental and the random coil C^{α} chemical shifts (ΔC^{α}) of free calmodulin (*A*,*D*), the calmodulin:SEF2-1mp complex (*B*,*E*), and the calmodulin:M13 complex (Ikura et al. 1991b; *C*,*F*). Panels *D*, *E*, and *F* are enlargements of the ΔC^{α} of the central helix (helix IV and V) of free calmodulin, the calmodulin:SEF2-1mp complex, and the calmodulin:M13 complex, respectively. The major differences in ΔC^{α} shifts are located in the central helix. Here the ΔC^{α} shifts of the free calmodulin (*D*) and the calmodulin:SEF2-1mp complex (*E*) closely follow each other while those of the calmodulin:M13 complex (*F*) are significantly different. This means that the calmodulin in the calmodulin:SEF2-1mp complex does not collapse into the wraparound binding mode as in the case of the calmodulin:M13 complex.

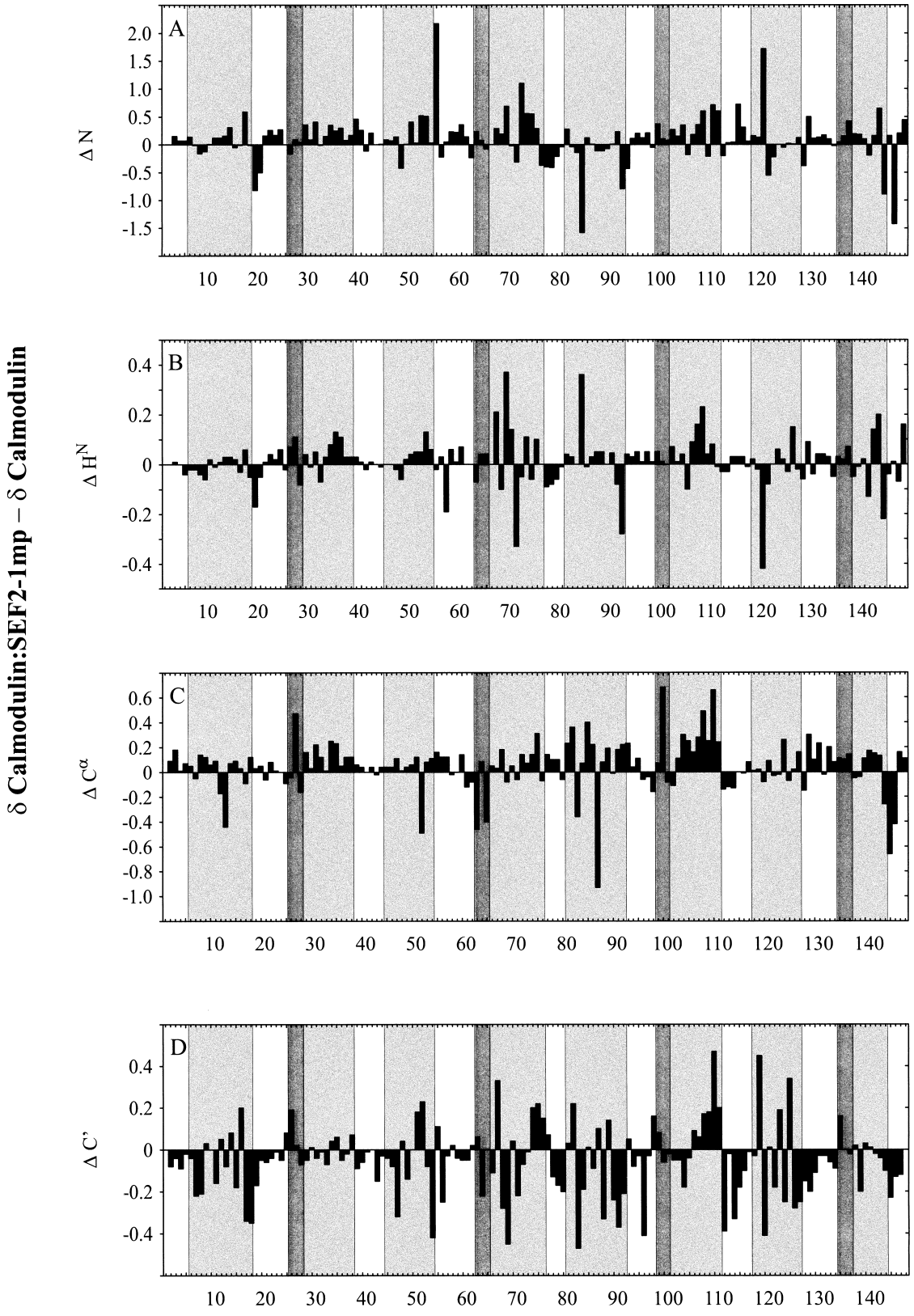

Fig. 7. Differences in the backbone chemical shifts between SEF2-1mp-bound calmodulin and free calmodulin. The light shaded and dark shaded areas are α-helices and β-sheets in the calmodulin:SEF2-1mp complex. Spectra of free and SEF2-1-bound calmodulin were recorded under the same conditions with the Bruker DRX 600 spectrometer.

fected when at least two of the following conditions hold, $|\Delta N| > \sim 0.5$ ppm, $|\Delta H^N| > 0.1$ ppm, $|\Delta C^\alpha| > 0.3$ ppm, and $|\Delta C'| > 0.3$ ppm. The affected residues in the N-terminal domain (13, 17, 19 27, 47, 48, 52, 53, 54, 55, 60, 61, 67, 69, 72, 73, 75) are lining the hydrophobic surface of the N-terminal domain and either are the same residues or are neighboring the residues that interact with M13 in the calmodulin:M13 complex (Ikura et al. 1992) or with CaMKK in the CaM:CaMKK complex (Osawa et al. 1999). The affected residues in the C-terminal domain (83, 84, 85, 87, 88, 91, 92, 108, 110, 111, 112, 114, 115, 120, 121, 129, 143, 144, 145, 146) also line the hydrophobic channel and correspond closely to the residues that show NOE contacts with the peptide in the calmodulin:M13 or CaM:CaMKK complexes. In conclusion, the chemical shift analysis shows that the same hydrophobic surfaces that interact with the target peptide in the wraparound binding mode are also involved in the SEF2-1mp interaction. This interaction is confirmed by NOE contacts seen in the three-dimensional F1 $^{13}C/^{15}N$-filtered, F2 $^{13}C/^{15}N$-edited NOESY spectrum (Fig. 5). First, relatively strong intermolecular NOE cross peaks are seen between the important methionine methyl groups and different residues in SEF2-1mp. Conversely, the strongest intermolecular NOE contacts of SEF2-1mp involve the hydrophobic residues Leu 13 and Val 15 close by or in the putative α-helix (Asn 7 to Arg 14) and methyl groups in the N- and C-terminal domains of calmodulin (Fig. 5B,C).

Although hydrophobic interactions discussed above play an important role in the calmodulin:SEF2-1mp interaction, hydrophobic calmodulin inhibitors, which are believed to bind to hydrophobic calmodulin patches, inhibit the SEF2-1-calmodulin interaction less efficiently than wraparound interactions (Onions et al. 2000). In addition, the calmodulin:SEF2-1 interaction was shown to be more salt sensitive than the wraparound calmodulin-peptide interactions. We find relatively strong NOEs from the H^δ protons of arginines in SEF2-1mp to calmodulin (Fig. 5A,D), indicating electrostatic interactions of the positively charged peptide with the negatively charged calmodulin surface. We conclude that electrostatic interactions play a larger role for SEF2-1mp than for other calmodulin-binding peptides. This is not surprising, as the sequence of SEF2-1 is highly charged with predominantly basic residues.

In conclusion, the calmodulin:SEF2-1mp complex represents a novel calmodulin binding mode. This conclusion is based on the following new findings: First, two calmodulin molecules bind one dimeric peptide; second, the two calmodulin molecules in the complex interact with each other (Met 36 in the N-domain of one calmodulin to Leu 112 in the C-domain of the other calmodulin); third, the binding does not occur via a wraparound binding mode but via a more open form (based on the secondary structure and exchange data), although the hydrophobic surfaces of the N- and C-terminal domains still form the main interaction sites; fourth, in the complex the peptide is not in a purely α-helical state; and fifth, the calmodulin:peptide interaction is in fast exchange on the NMR timescale. Figure 8 summarizes the main aspects of the novel binding motif of calmodulin and the dimeric SEF2-1mp in a schematic cartoon representation of two alternative structures as derived from the NMR data presented in this study. The full structure determination of the calmodulin:SEF2-1mp complex is currently in progress.

Materials and methods

Sample preparations

Recombinant calmodulin with the mammalian amino acid sequence was overexpressed in *Escherichia coli* strain BL21(DE3) pLysS as previously described (Onions et al. 1997). Uniform ^{15}N or $^{15}N/^{13}C$ labeling was obtained by growing the bacteria in M9 minimal media containing 0.1% ^{15}N-ammonium chloride or 0.2% ^{13}C-glucose and 0.1% ^{15}N-ammonium chloride. The recombinant calmodulin was purified as previously described (Onions et al. 1997).

A 21-residue-long peptide was purchased from Saveen. Purity of the peptide was >95%, as determined by HPLC and mass spectroscopy. The peptide sequence is **KERRMANNARERLRVR**G GCGW, where the amino acids in bold correspond to the basic region (residue 563–578) in the bHLH domain of SEF2-1. The five C-terminal residues in the linker provide a flexible dimerization region, which includes a tryptophan for fluorescence measurements. Diamide (azodicarboxylic acid bis(dimethylamide)) was subsequently used to oxidize the cysteine in the linker region, thereby forcing the peptide to dimerize.

The ^{15}N-calmodulin:SEF2-1mp as well as the $^{13}C/^{15}N$-calmodulin:SEF2-1mp complexes were identically made as below. Approximately 13 mg lyophilized Ca^{2+} free calmodulin was dissolved in 25 mL of 0.32 mM $CaCl_2$, 4.0 mM KCl, and 4 μM NaN_3. The solution was lyophilized. Ca^{2+}-loaded freeze-dried CaM was resuspended in 1 mL of water and 1 mL of NMR solution (100 mM KCl, 8 mM $CaCl_2$, 0.1 mM NaN_3, 4 mM diamide, and 10% D_2O). The protein solution was further washed with 7 mL NMR solution over a centricon 10 filter (amicon, 10-kD cut off) and finally concentrated to 500 μL.

Roughly 2 mg of the SEF2-1mp peptide was dissolved in 1.5 mL of NMR solution and washed and concentrated as the calmodulin with the exception that the concentration unit now was an micropartition filter unit (amicon) equipped with a YM1 filter (amicon, 1-kD cut off). The pH of the calmodulin and peptide samples was adjusted to 6.0 with either diluted HCl or KOH. Concentrations of the calmodulin and the peptide were estimated by UV spectroscopy. A 1.0 mM CaM:SEF2-1 complex in 500 μL was made by adding the two solutions in appropriate volumes followed by concentration with a micropartition filter unit. A Tricine SDS-PAGE without any reducing agents in the loading buffer verified that the peptide was in the dimeric state.

NMR experiments

All NMR experiments were performed at 35°C when not indicated otherwise. The NMR experiments were either performed on a Bruker DRX-600 or a Bruker AMX2-500 spectrometer equipped

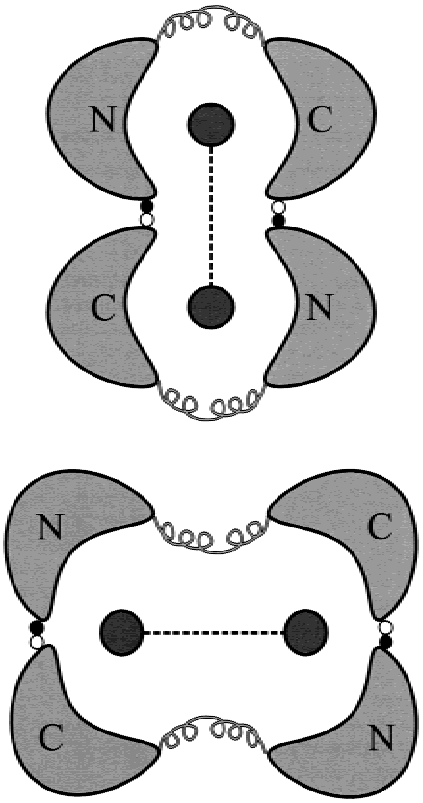

Fig. 8. Two cartoon presentations of alternative structures of the calmodulin:SEF2-1mp complex that are consistent with the presently derived NMR data, summarized at the end of the discussion. In the top presentation, one monomer of the dimeric peptide interacts with the N and C domains of the same calmodulin. In the bottom presentation, this interaction is with the N and C domain of different calmodulin molecules. Amino acids Met 36 and Leu 112 making intermolecular calmodulin:calmodulin contacts are indicated as filled and open circles, respectively. The two presentations are drawn in a plane, but the two interacting calmodulin molecules may also interact at an angle. At this point, we cannot distinguish between these different conformations.

with triple resonance (^{1}H/^{13}C/^{15}N) or (^{1}H/^{13}C/broadband) probes with XYZ-gradient capabilities. Quadrature detection in the indirect dimensions was obtained by States-TPPI (Marion et al. 1989). If gradient enhancement was used, quadrature detection was obtained by the echo/antiecho method (Kay et al. 1992; Schleucher et al. 1994). Before Fourier transformation, linear predictions were applied in all indirect dimensions and the time domain data were zero filled and apodized by a phase-shifted squared sine bell (processing software, XWINNMR).

All ^{1}H dimensions were referenced to internal DSS. ^{13}C and ^{15}N dimensions were calibrated using the magnetogyro ratios ^{15}N/^{1}H = 0.101329118 and ^{13}C/^{1}H = 0.251449530 (Wishart et al. 1995a). All data analysis and cross-peak integration were made using the software SYBYL (TRIPOS). NMR experiments and the corresponding parameters used in the resonance assignment of calmodulin in the calmodulin:SEF2–1mp complex are compiled in Table 1.

To be able to compare the backbone chemical shifts of free and SEF2-1mp-bound calmodulin, the backbone chemical shifts of free calmodulin were reassigned at the same conditions as the calmodulin:SEF2-1mp complex. This was done with the triple resonance experiments CBCANH, CBCACONH, and HNCO, which were recorded at the BRUKER 600 MHz DRX spectrometer.

The stoichiometry of the complex was determined in a titration experiment where increasing amounts of calmodulin were added to a fixed amount of SEF2-1mp. Four titration points corresponding to calmodulin:SEF2-1mp molar ratios of 0.5 : 1, 1 : 1, 2 : 1, and 2.3 : 1 were analyzed by following the peak positions in ^{15}N-HSCQ spectra measured at 500 MHz ^{1}H frequency. The bulk calmodulin concentration in the titration experiment was 2.3 mM, and the start concentration for SEF2-1mp before any calmodulin addition was 1.125 mM. One reference point for free calmodulin under the same conditions was also recorded.

The assignment of SEF2-1mp was achieved by a combination of two-dimensional ^{13}C and ^{15}N isotope-filtered TOCSY and NOESY experiments. Both the NOESY and TOCSY experiments were recorded as 1024×280 complex matrices at 600 MHz ^{1}H frequency. The NOESY experiments had 64 scans per complex t_1 point, and the TOCSY experiments had 48 scans per complex t_1 point. In the NOESY experiments, the isotope filter by Zwahlen et al. (1997) was applied before t_1 and the isotope filter suggested in the review of Sattler et al. (1999) was applied prior to t_2. Three different NOESY mixing times (80, 120, and 180 msec) were used in the doubly filtered NOESY experiment. The only filter used in the TOCSY experiments was the ^{13}C/^{15}N isotope filter from Zwahlen et al. (1997), and it was applied before t_1. The mixing time used in the TOCSY step was 75 msec. To make a complete assignment of the calmodulin-bound SEF2-1mp, both the isotope-filtered NMR experiments were carried out at 15°, 25°, and 35°C.

Homonuclear $^3JH^NH^\alpha$ coupling constants for calmodulin were derived from a three-dimensional ^{15}N-separated quantitative J-correlation HNHA spectrum (Vuister and Bax 1993). The spectrum was recorded on the DRX 600 spectrometer with sweep widths of 7183, 5905, and 1398 Hz for the ^{1}H acquisition dimension, the ^{1}H indirect dimension, and the ^{15}N dimension, respectively. The size of the final data matrix was $1536 \times 120 \times 100$ complex points for the ^{1}H, ^{1}H, and ^{15}N dimensions. Before Fourier transformation, the data matrix was linear predicted in the indirect dimensions and zero filled to a final size of $2048 \times 256 \times 256$ complex points. The de- and refocusing delay, ζ, was set to 13.05 msec according to Vuister and Bax (1993). $^3JH^NH^\alpha$ couplings were derived by fitting the ratio between the diagonal peak intensity, S_{diag}, and the H^NH^α cross-peak intensity, S_{cross}, to the equation

$$\frac{S_{cross}}{S_{diag}} = -\tan^2(2\pi J_{HH\xi}) \quad (1)$$

The fitting to equation (1) was made in the software MATLAB. Because of different relaxation properties of the in-phase H^N-H^N diagonal peak and the antiphase and the H^N-H^α cross peak during the de- and refocusing delay 2ζ, the derived $^3JH^NH^\alpha$ couplings were corrected by a correction factor of 1.11, as described by Vuister and Bax (1993).

The computer program TALOS (Cornilescu et al. 1999) is designed to predict protein backbone angles (ϕ,ψ) by searching for similarities in chemical shifts for homologous residues in a database containing C^α, C^β, C', H^α, and N chemical shifts and high-resolution X-ray structures. This computer software was used in the prediction of the backbone ϕ and ψ angles for calmodulin based on the calmodulin assignment in the calmodulin:SEF2-1mp complex.

NOE contacts between calmodulin and SEF2-1mp were derived from a three-dimensional F1 ^{13}C/^{15}N-filtered, F2 ^{13}C/^{15}N-edited NOESY (Zwahlen et al. 1997). The spectrum was recorded on the DRX 600 MHz spectrometer at 35°C with sweep widths of 8389,

5433, and 7321 Hz for the ^{1}H, $^{13}C/^{15}N$, and ^{1}H, respectively. The size of the data matrix was $1536 \times 90 \times 188$ complex points and was zero filled to $2048 \times 128 \times 256$ complex points for the ^{1}H, $^{13}C/^{15}N$, and ^{1}H dimensions, respectively. Linear prediction was applied for the two indirect dimensions, and the data matrix was apodized by a phase-shifted squared sine bell function before Fourier transformation.

A 1 : 1 : 2 complex of doubly labeled calmodulin, unlabeled calmodulin, and SEF2-1mp was made to investigate if any intermolecular calmodulin:calmodulin contacts were present in the complex. The final NMR sample consisted of 0.7 mM of each calmodulin and 1.4 mM of the SEF2-1mp. To detect any intermolecular calmodulin contacts, a three-dimensional F1 $^{13}C/^{15}N$-filtered, F2 $^{13}C/^{15}N$-edited NOESY was recorded. The same spectral parameters were used as for the calmodulin:SEF2-1mp isotope-filtered NOESY described above. Cross peaks that are absent in the X-filtered spectrum in the 1 : 1 complex of doubly labeled calmodulin:SEF2-1mp but present here are calmodulin:calmodulin contacts. These cross peaks should also fulfil another condition that distinguishes them from calmodulin:peptide interactions. The calmodulin:calmdulin contacts are symmetrical with respect to their origin. A contact from proton HA in labeled calmodulin to proton HB in unlabeled calmodulin is accompanied by a contact from HB in labeled calmodulin to HA in unlabeled calmodulin. Consequently, calmodulin:calmodulin contacts are easily identified in the ^{1}H (F1), ^{1}H (F3) projection, where they show up as symmetrical cross peaks. In contrast, calmodulin:peptide contacts are not symmetrical in this projection.

The apparent exchange rate, R_{ex}*, of rapidly exchanging amide protons can be estimated from the ratios of intensities between the diagonal peak (I_{diag}) and the cross peak at the water frequency ($I_{H_2}0$) in the ^{15}N-edited NOESY:

$$R_{ex}* = -\ln\left(\frac{I_{diag}}{I_{diag+I_{H_2O}}}\right) \Big/ T_{mix} \qquad (2)$$

where Tmix is the NOESY mixing time. Equation (2) disregards the magnetization transfer into other cross-peak positions, and consequently, R_{ex}* is slightly overestimated (maximum error is ~20). Apart from the actual exchange rate (R_{ex}), the apparent exchange rate (R_{ex}*) can also contain contributions from NOE transfer (R_{NOE}), that is, $R_{ex}* = R_{ex} + R_{NOE}$ (Spera and Ikura 1991). Because of the pH dependence of R_{ex}, one can distinguish the two rates by measuring at different pH values. This was not done here because R_{NOE} generally makes a small contribution, as was shown by Spera and Ikura (1991) for the calmodulin:M13 complex and free calmodulin. Consequently, R_{ex}* can be used to estimate R_{ex} at least semiqualitatively, with R_{ex}* being equal or slightly larger than R_{ex}.

Acknowledgments

This work was supported by grants from the Swedish National Science Research Council (S.W.), the Bioteknik Medel Umeå University (S.W.), the Swedish Research Council for Engineering Sciences/SSF (T.G.), and the Kempe Foundation (G.L.).

The publication costs of this article were defrayed in part by payment of page charges. This article must therefore be hereby marked "advertisement" in accordance with 18 USC section 1734 solely to indicate this fact.

References

Babu, Y.S., Bugg, C.E., and Cook, W.J. 1988. Structure of calmodulin refined at 2.2 å resolution. *J. Mol. Biol.* **204:** 191–204.

Barbato, G., Ikura, M., Kay, L.E., Pastor, R.W., and Bax, A. 1992. Backbone dynamics of calmodulin studied by N-15 relaxation using inverse detected 2-dimensional NMR-spectroscopy—The central helix is flexible. *Biochemistry* **31:** 5269–5278.

Chattopadhyaya, R., Meador, W.E., Means, A.R., and Quiocho, F.A. 1992. Calmodulin structure refined at 1.7 angstroms resolution. *J. Mol. Biol.* **228:** 1177–1192.

Corneliussen, B., Holm, M., Waltersson, Y., Onions, J., Hallberg, B., Thornell, A., and Grundström, T. 1994. Calcium/calmodulin inhibition of basic-helix–loop–helix transcription factor domains. *Nature* **368:** 760–764.

Cornilescu, G., Delaglio, F., and Bax, A. 1999. Protein backbone angle restraints from searching a database for chemical shift and sequence homology. *J. Biolmol. NMR* **13:** 289–302.

Dash, P.K., Karl, K.A., Colicos, M.A., Prywes, R., and Kandel, E.R. 1991. Camp response element-binding proteins is activated by Ca^{2+}/calmodulin-dependent as well mas camp-dependent protein-kinase. *Proc. Natl. Acad. Sci.* **88:** 5061–5065.

Ellenberger, T., Fass, D., Arnaud, M., and Harrison, S.C. 1994. Crystal-structure of transcription factor E47—E-box recognition by a basic region helix–loop–helix dimer. *Genes & Dev.* **8:** 970–980.

Elshorst, B., Hennig, M., Försterling, H., Dienner, A., Maurer, M., Schulte, P., Schwalbe, H., Griesinger, C., Krebs, J., Schmid, H., et al. 1999. NMR solution structure of a complex of calmodulin with a binding peptide of the Ca^{2+} pump. *Biochemistry* **38:** 12320–12332.

Fairman, R., BeranSteed, R.K., and Handel, T.M. 1997. Heteronuclear (H-1,C-13,N-15) NMR assignments and secondary structure of the basic region-helix–loop–helix domain of E47. *Prot. Sci.* **6:** 175–184.

Finn, B.E., Evenäs, J., Drakenberg, T., Waltho, J.P., Thulin, E., and Forsen, S. 1995. Calcium-induced structural-changes and domain autonomy in calmodulin. *Nat. Struct. Biol.* **2:** 777–783.

Grzesiek, S. and Bax, A. 1992. Correlating backbone amide and side-chain resonances in larger proteins by multiple relayed triple resonance NMR. *J. Am. Chem. Soc.* **114:** 6291–6293.

———. 1993. Amino-acid type determination in the sequential assignment procedure of uniformly $^{13}C/^{15}N$-enriched proteins. *J. Biolmol. NMR* **3:** 185–204.

Houdusse, A., Silver, M., and Cohen, C. 1996. A model of Ca^{2+}-free calmodulin binding to unconventional myosins reveals how calmodulin acts as a regulatory switch. *Structure* **4:** 1475–1490.

Ikura, M. 1996. Calcium binding and conformational response in EF-hand proteins. *Trends Biochem. Sci.* **21:** 14–17.

Ikura, M., Spera, S., Barbato, G., Kay, L.E., Krinks, M., and Bax, A. 1991a. Secondary structure and side-chain H-1 and C-13 resonance assignment of calmodulin in solution by heteronuclear multidimensional NMR spectroscopy. *Biochemistry* **30:** 9216–9228.

Ikura, M., Kay, L.E., Krinks, M., and Bax, A. 1991b. Triple-resonance multidimensional NMR study of calmodulin complexed with the binding domain of skeletal muscle myosin light-chain kinase: Induction of a conformational change in the central helix. *Biochemistry* **30:** 5498–5504.

Ikura, M., Clore, G.M., Gronenborn, A.M., Zhu, G., Klee, C.B., and Bax, A. 1992. NMR solution structure of a calmodulin-target peptide complex by multidimensional. *Science* **256:** 632–638.

James, P., Vorherr, T., and Carafoli, E. 1995. Calmodulin-binding domains—Just 2-faced or multifaceted. *Trends Biochem. Sci.* **20:** 38–42.

Jurado, L.A., Chockalingam, P.S., and Jarret, H.W. 1999. Apocalmodulin. *Physiol. Rev.* **79:** 661–682.

Kapiloff, M.S., Mathis, J.M., Nelson, C.A., Lin, C.R., and Rosenfeld, M.G. 1991. Calcium calmodulin-dependent protein-kinase mediates a pathway for transcriptional regulation. *Proc. Natl. Acad. Sci.* **88:** 3710–3714.

Kay, L.E., Keifer, P., and Saarinen, T. 1992. Pure absorption gradient enhanced heteronuclear single quantum correlation spectroscopy with improved sensitivity. *J. Am. Chem. Soc.* **114:** 10663–10665.

Klee, C.B. and Krinks, M.H. 1978. Purification of cyclic 3′,5′-nucleotide phosphodiesterase inhibitory protein by affinity chromatography on activator protein coupled to Sepharose. *Biochemistry* **17:** 120–126.

Kuboniwa, H., Tjandra, N., Grzesiek, S., Ren, H., Klee, C.B., and Bax, A. 1995. Solution structure of calcium-free calmodulin. *Nat. Struct. Biol.* **2:** 768–776.

Larsson, G., Wijmenga, S.S., and Schleucher, J. 1999. A high-resolution HCANH experiment with enhanced sensitivity via multiple quantum line narrowing. *J. Biolmol. NMR* **14:** 169–174.

Littlewood, T.D. and Evan, G.I. 1998. *Helix–loop–helix transcription factors.* Oxford University Press, Oxford.

Ma, P.C.M., Rould, M.A., Weintraub, H., and Pabot, C.O. 1994. Crystal-structure of MyoD bHLH domain-DNA complex—Perspectives on DNA recognition and implications for transcriptional activation. *Cell* **77:** 451–459.

Marion, D., Ikura, M., Tschudin, R., and Bax, A. 1989. Rapid recording of 2D

NMR-spectra without phase cycling—Application to the study of hydrogen-exchange in proteins. *J. Magn. Reson.* **85:** 393–399.
Massari, M.E. and Murre, C. 2000. Helix–loop–helix proteins: Regulators of transcription in eucaryotic organisms. *Mol. Cell. Biol.* **20:** 429–440.
Meador, W.E., Means, A.R., and Quiocho, F.A. 1992. Target enzyme recognition by calmodulin—2.4-angstrom structure of calmodulin-peptide complex. *Science* **257:** 1251–1255.
Mirzoeva, S., Weigand, S., Lukas, T.J., Shuvalova, L., Andersson, W.F., and Watterson, D.M. 1999. Analysis of the functional coupling between calmodulin's calcium binding and peptide recognition properties. *Biochemistry* **38:** 3936–3947.
Montelione, G.T., Lyons, B.A., Emerson, S.D., and Tashiro, M. 1992. An efficient triple resonance experiment using ^{13}C isotropic mixing for determining sequence-specific resonance assignment of isotropically-enriched proteins. *J. Am. Chem. Soc.* **114:** 10974–10975.
Oneil, K.T. and Degrado, W.F. 1990. How calmodulin binds its targets—Sequence independent recognition of amphiphilic α-helices. *Trends Biochem. Sci.* **15:** 59–64.
Onions, J., Hermann, S., and Grundström, T. 1997. Basic helix–loop–helix protein sequences determining differential inhibition by calmodulin and S-100 proteins. *J. Biol. Chem.* **272:** 23930–23937.
Onions, J., Hermann, S., and Grundström, T. 2000. A novel type of calmodulin interaction in the inhibition of basic Helix–loop–helix transcription factors. *Biochemistry* **39:** 4366–4374.
Osawa, M., Tokumitsu, H., Swindells, M.B., Kurihara, H., Orita, M., Shibanuma, T., Furuya, T., and Ikura, M. 1999. A novel target recognition revealed by calmodulin in complex with Ca^{2+}-calmodulin-dependent kinase kinase. *Nat. Struct. Biol.* **6:** 819–824.
Phillips, S.E.V. 1994. Built by association—Structure and function of helix–loop–helix DNA-binding proteins. *Structure* **2:** 1–4.
Sattler, M., Schleucher, J., and Griesinger, C. 1999. Heteronuclear multidimensional NMR experiments for the structure determination of proteins in solution employing pulsed field gradients. *Prog. Nucl. Magn. Reson. Spectro.* **34:** 93–158.
Saudek, V., Pasley, H.S., Gibson, T., Gausepohl, H., Frank, R., and Pastore, A. 1991. Solution structure of the basic region from the transcriptional activator GCN4. *Biochemistry* **30:** 1310–1317.
Schleucher, J., Schwendinger, M., Sattler, M., Schmidt, P., Schedletzky, O., Glaser, S.J., Sorensen, O.W., and Griesinger, C. 1994. A general enhancement scheme in heteronuclear multidimensional NMR employing pulsed-field gradients. *J. Biolmol. NMR* **4:** 301–306.
Sheng, M., Thompson, M.A., and Greenberg, M.E. 1991. Creb—A Ca^{2+}-regulated transcription factor phosphorylated by calmodulin-dependent kinase. *Science* **252:** 1427–1430.
Spera, S. and Ikura, M. 1991. Measurement of the exchange rates of rapidly exchanging amide protons: Application to the study of calmodulin and its complex with a myosin light chain kinase fragment. *J. Biolmol. NMR* **1:** 155–165.
Stewart, A.A., Ingebritsen, T.S., Manalan, A., Klee, C.B., and Cohen, P. 1982. Discovery of a Ca^{2+}- and calmodulin-dependent protein phosphatase: Probable identity with calcineurin (CaM-BP80). *FEBS Lett.* **137:** 80–84.
Van Eldik, L. and Watterson, D.M. 1998. *Calmodulin and signal transduction.* Academic Press.
Vuister, G.W. and Bax, A. 1993. Quantitative J correlation—A new approach for measuring homonuclear 3-bond J(H(N)H(α)) coupling-constants in N-15 enriched proteins. *J. Am. Chem. Soc.* **115:** 7772–7777.
Waltersson, Y., Linse, S., Brodin, P., and Grundström, T. 1993. Mutational effects on the cooperativity of Ca^{2+} binding in calmodulin. *Biochemistry* **32:** 7866–7871.
Wegner, M., Cao, Z.D., and Rosenfeld, M.G. 1992. Calcium-regulated phosphorylation within the leucine zipper of C/EBP-β. *Science* **256:** 370–373.
Wishart, D.S., Sykes, B.D., and Richards, F.M. 1991. Relationship between nuclear-magnetic-resonance chemical-shift and protein secondary structure. *J. Mol. Biol.* **222:** 311–333.
Wishart, D.S., Bigam, C.G., Yao, J., Abildgaard, F., Dyson, H.J., Oldfield, E., Markley, J.L., and Sykes, B.D. 1995a. H-1, C-13 and N-15 chemical-shift referencing in biomolecular NMR. *J. Biolmol. NMR* **6:** 135–140.
Wishart, D.S., Bigam, C.G., Holm, A., Hodges, R.S., and Sykes, B.D. 1995b. ^{1}H, ^{13}C and ^{15}N random coil shifts of common amino acids: Investigation of nearest-neighbour effects. *J. Biomol. NMR* **5:** 67–81.
Yamazaki, T., Forman-Kay, J.D., and Kay, L.E. 1993. 2-Dimensional NMR experiments for correlating C-13-β and H-1-δ/ϵ chemical-shifts of aromatic residues in C-13 labeled proteins via scalar couplings. *J. Am. Chem. Soc.* **115:** 11054–11055.
Yuan, T. and Vogel, H.J. 1998. Calcium-calmodulin-induced dimerization of the carboxyl-terminal domain from petunia glutamate decarboxylase. *J. Biol. Chem.* **273:** 30328–30335.
Zhang, M., Tanaka, T., and Ikura, M. 1995. Calcium-induced conformational transitional transition revealed by the solution structure of apo calmodulin. *Nat. Struct. Biol.* **2:** 758–767.
Zwahlen, C., Legault, P., Vincent, S.J.F., Greenblatt, J., Konrat, R., and Kay, L.E. 1997. Methods for measurement of intermolecular NOEs by multinuclear NMR spectroscopy: Application to a bacteriophage λ N- peptide/boxB RNA complex. *J. Am. Chem. Soc.* **119:** 6711–6721.